A closed-form shear resistance model for regions of prestressed beams without flexural cracks

Roosen, Marco A.; Yang, Yuguang; van der Veen, Cor; Schaafsma, Dick G.; Hendriks, Max A.N.

DOI
10.1002/suco.202100695

Publication date
2022

Document Version
Final published version

Published in
Structural Concrete

Citation (APA)
Roosen, M. A., Yang, Y., van der Veen, C., Schaafsma, D. G., & Hendriks, M. A. N. (2022). A closed-form shear resistance model for regions of prestressed beams without flexural cracks. *Structural Concrete*, *23*(3), 1304-1315. https://doi.org/10.1002/suco.202100695

Received: 4 October 2021 | Revised: 17 December 2021 | Accepted: 17 January 2022

DOI: 10.1002/suco.202100695

ARTICLE

fib CEB-FIP WILEY

A closed-form shear resistance model for regions of prestressed beams without flexural cracks

Marco A. Roosen[1,2] | **Yuguang Yang**[2] | **Cor van der Veen**[2] | **Dick G. Schaafsma**[1] | **Max A. N. Hendriks**[2,3]

[1]Dutch Ministry of Infrastructure and Water Management, Utrecht, The Netherlands

[2]Delft University of Technology (TU Delft), Delft, The Netherlands

[3]Norwegian University of Science and Technology (NTNU), Trondheim, Norway

Correspondence
Marco A. Roosen, Rijkswaterstaat, Griffioenlaan 2, 3526 LA, Utrecht, The Netherlands.
Email: marco.roosen@rws.nl

Abstract

When the shear resistance of prestressed beams with stirrups is determined with the current Eurocode, no distinction is made between regions with and without flexural cracks. This while it may be expected that a region without flexural cracks will have a higher shear resistance. This is due to the lower longitudinal strains and the narrow crack widths, resulting in a higher contribution of aggregate interlock. Also, the Eurocode does not take into account that in regions without flexural cracks, a significant part of the shear force is transferred through the uncracked flanges. This article proposes therefore a shear resistance model, based on Modified Compression Field Theory (MCFT), that does consider the low longitudinal strains and shear transfer through the uncracked flanges. From a comparison it was found that the proposed model can determine shear resistance as accurately as the most comprehensive level III approach of the Model Code 2010. However, the proposed model was found to be much easier to use in engineering practice as no iterations are necessary.

KEYWORDS

existing structures, prestressed concrete, regions without flexural cracks, shear resistance, web-shear failure

1 | INTRODUCTION

A significant part of the concrete bridges in the Dutch Highway network contains stirrups and is prestressed. When carrying out structural assessments, it is frequently found that the shear resistance of these prestressed structures is insufficient, especially in the regions around the end supports. On the other hand, in these regions no flexural cracks are present in the flanges due to the prestressing present, so that the longitudinal strains are low. Due to the low longitudinal strains, the possible crack widths in the web will be small, so that the contribution of the aggregate interlock to the shear resistance will be significant. Moreover, a considerable part of the shear force will be transferred through the flanges because they remain uncracked. These phenomena are not included in the models used in the Eurocode[1] or the additional Dutch

Discussion on this paper must be submitted within two months of the print publication. The discussion will then be published in print, along with the authors' closure, if any, approximately nine months after the print publication.

assessment guideline.[2] It is therefore unclear whether the shear resistance of the assessed bridges is really too low.

Therefore, it was first evaluated whether these issues can be solved with well-known existing shear resistance models. This concerns, in addition to the variable angle truss model[3] as used in the Eurocode,[1] other models such as an empirical model derived by MacGregor et al.[4] as used in ACI,[5] arch action models combined with truss analogy as used in the Model Code 1990[6] and models based on the MCFT as used in the Model Code 2010[7] and the CSA.[8] None of these models distinguish between shear resistance in regions with and without flexural cracks. This is apparent from the observation that all these models relate the shear resistance to the effective depth of the prestressing and reinforcing steel. While this is a suitable assumption for regions with flexural cracks, it is not for regions without flexural cracks. This is because the prestressing and reinforcing steel are located in the uncracked flange, making the location irrelevant for the shear resistance. On the other hand, the models based on the MCFT are strain-based and therefore do take into account the higher aggregate interlock in regions without flexural cracks. However, a disadvantage of these current strain-based models is that the use is laborious because many comparisons and iteration steps are required to determine the shear resistance.

This article therefore proposes a closed-form, strain-based shear resistance model that is suitable to determine the shear resistance in the regions without flexural cracks. The work is based on a recently published dissertation[9] at Delft University of Technology. In addition to the PhD research, this article compares the proposed model with the Level III approach as described in the Model Code 2010.

2 | SHEAR TRANSFER MECHANISMS IN REGIONS WITHOUT FLEXURAL CRACKS

Figure 1 shows a free-body diagram for a region without flexural cracks and with diagonal tension cracks. Diagonal tension cracks occur when the maximum principal tensile stress in the web is equal to the tensile strength of concrete. The diagonal stress crack can then open further. This is possible, despite the longitudinal strains being approximately zero, due to the increase in transverse strains. This is for instance observed in strain measurements of ε_z in experiments that failed in a region without flexural cracks performed by Rupf.[10]

Along the edge of the free-body diagram, shear force can be transmitted by three mechanisms:

1. Shear transfer along the diagonal tension crack by stirrups crossing the diagonal tension crack, as shown in the left part of Figure 1. The shear force that is resisted by the stirrups ($V_{R,s}$) equals the number of stirrups crossing the crack ($z_{cr}\ \cot\theta/s$) multiplied by the force in the stirrups ($A_{sw}\ \sigma_{w,cr}$). In these equations, z_{cr} is the cracked height, θ is the angle of the crack, s is the distance between the stirrups, $\sigma_{w,cr}$ the stress in the stirrups in the crack and A_{sw} the area of shear reinforcement. The shear force resisted by the stirrups can also be expressed as a distributed stress, τ_s, by dividing $V_{R,s}$ by z_{cr} and the cross-sectional width b_z. In this way a τ_s that equals to $\rho_z\ \sigma_{w,cr}\ \cot\theta$ is found, in which ρ_z denotes the ratio of reinforcing steel in z direction.
2. Shear transfer by aggregate interlock stresses, τ_{ci}, along the diagonal tension crack, as shown in the right part of Figure 1. The shear force that can be resisted by aggregate interlock ($V_{R,ci}$) can be found by integrating τ_{ci} over the cross-sectional width (b_z) and the cracked height (z_{cr}).
3. Shear transfer by shear stresses in the uncracked concrete, τ_{uncr}, above and below the diagonal tension crack, as shown in the right part of Figure 1. The shear force that can be resisted by the uncracked parts ($V_{R,uncr}$) can be found by integrating τ_{uncr} over the cross-sectional width (b_z) and the uncracked height (z_{uncr}).

The vertical component of prestress is not considered a shear transfer mechanism because this article assumes

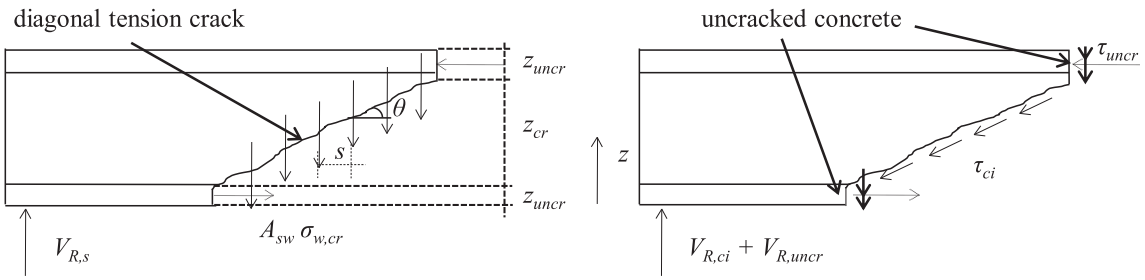

FIGURE 1 Possible shear transfer mechanism for a girder with stirrups in regions without flexural cracks

the equivalent prestressing method, where prestress is considered a load.

3 | SHEAR FAILURE MODES IN REGIONS WITHOUT FLEXURAL CRACKS

In regions without flexural cracks, two possible failure modes of the web are distinguished, namely slipping of the crack while the stirrups are yielding and crushing of the concrete while the stirrups are yielding. For very large amounts of shear reinforcement, it would theoretically also be possible for the concrete to crush without the stirrups yielding. It is noted that the Model Code 2010 (MC2010) distinguishes these same failure modes.[11]

The shear failure modes are investigated by using *Response*,[12] which is a nonlinear sectional analysis program based on the MCFT.[13] The MCFT is a theory capable of determining the load-deformation response of a membrane. Since the MCFT describes the behavior of reinforced concrete subjected to shear and normal in-plane stresses, it is also suitable to determine the resistance of the web of a beam. Moreover, since the longitudinal strain is a parameter in the MCFT, it is possible to account for the low longitudinal strain and its effect on the aggregate interlock. In addition to the MCFT, *Response* assumes that the beam theory is valid and that no transverse stresses are present.

The first failure mode to be investigated is the slipping of the crack and the simultaneous yielding of the stirrups. For this, a *Response* analysis was performed for beam HX1-A, which was part of a series of experiments by Hanson.[14] Figure 2 shows the contribution of shear transfer mechanism and associated parameters for the load step at which the maximum shear resistance is found. In this figure, τ_{ci} is the shear stress on the crack surface by aggregate interlock, w is the crack width, $\sigma_{w,cr}$ is the stress in the stirrups, θ is the angle of the crack, b_z is the width of the cross-section and τ_R is the total shear stress that can be resisted according to *Response*. Slipping of the crack is the governing failure mode because the maximum shear resistance is found at the load step at which τ_{ci} equals $\tau_{ci,max}$. It is noted that the stirrups yield at the crack width where τ_{ci} equals $\tau_{ci,max}$.

At the maximum shear force, the associated stresses in the compression field (σ_2) are not governing for this girder, as these are smaller than the maximum ($\sigma_{2,max}$) as shown in Figure 3.

The light gray area in Figures 2 and 3 show the part of the cross-section that is cracked and the dark gray areas show the uncracked parts. Because the longitudinal stresses are affected by the bending moment, a small part in the top of the web remains uncracked, whereas a small part of the skew bottom flange is cracked.

The added contributions of aggregate interlock and stirrups ($b_z\,\tau_R$) were found to be rather constant over the cracked height (Figure 2). It is noted that, despite that the maximum cracks width is decisive for the shear resistance at crack sliding, the distribution of the aggregate interlock stresses is not affected by the distribution of the crack width, as for this failure mode the crack width only determines $\tau_{ci,max}$. The stresses of the stirrups at the crack ($\sigma_{w,cr}$) were found to be equal to the yielding strength (f_{ywm}). Figure 2 also shows that the crack angle θ is rather constant over the cracked height. Only at the cracked part of the bottom flange the crack angle is

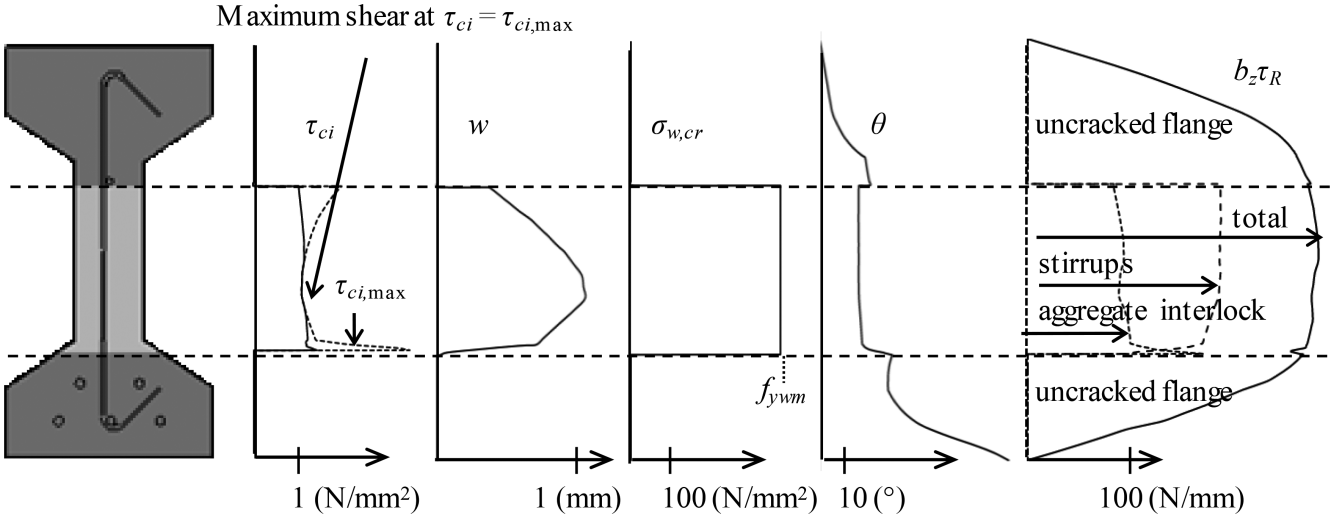

FIGURE 2 Contribution of shear transfer mechanism at failure of experiment HX1-A[14]

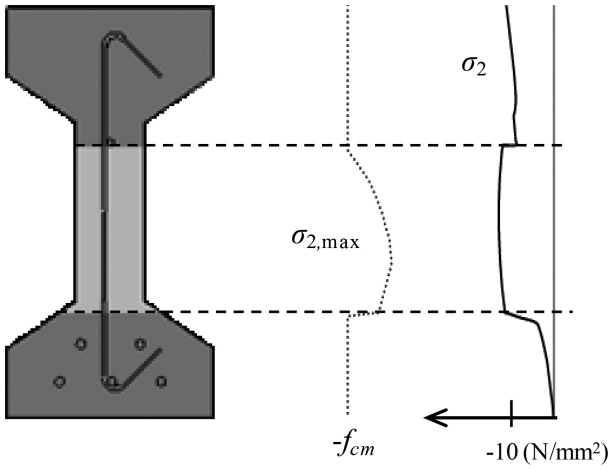

FIGURE 3 Stresses and maximum stresses in compression field at failure of HX1-A[14]

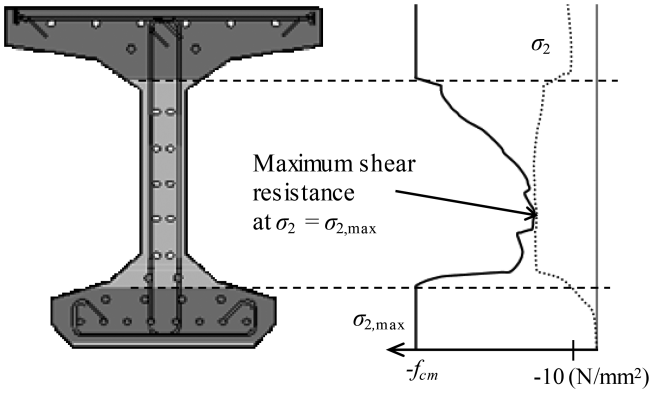

FIGURE 4 Stresses and maximum stresses in compression field at failure of HCP1TE[15]

higher than average, what causes a decrease in the contribution of the stirrups. On the other hand, for the total resistance $b_z\ \tau_R$, this decrease is compensated by an increase in the contribution of the aggregate interlock due to the increasing width of the cross-section.

The second failure mode under investigation is crushing in the compression field and simultaneously yielding of the stirrups. For this, a *Response* analysis was performed on beam HCP1TE, which was part of a series of experiments by Choulli.[15] Figure 4 shows the stresses in the compression field (σ_2) and the maximum allowable compressive stresses in the compression field ($\sigma_{2,max}$) at the load step where the maximum shear force was found. Crushing of the concrete is the governing failure mode because the maximum shear resistance is found at the load step at which σ_2 equals $\sigma_{2,max}$.

Figure 5 shows the contribution of shear transfer mechanism at failure and associated parameters for HCP1TE. As with beam HX1-A, the cracked area extends more into the bottom of the cross-section than the top, because the moment affects the longitudinal stresses.

Also for this failure mode, both the added contributions of aggregate interlock and stirrups ($b_z\ \tau_R$) were found to be rather constant over the cracked height (Figure 5). In contrast to the girder HX1-A, the girder HCP1TE could resist additional shear force after $\tau_{ci} = \tau_{ci,max}$. As a consequence, w is decisive for the distribution of τ_{ci} for a considerable part of the cross-section (height over which $\tau_{ci} = \tau_{ci,max}$), as shown in Figure 5. As for beam HX1-A, the decrease in the contribution of the stirrups in the lower flange due to the decrease in the crack angle is compensated by an increase in the contribution of the aggregate lock due to the increasing width of the cross-section.

4 | DERIVATION OF A CLOSED-FORM SHEAR RESISTANCE MODEL

4.1 | Mean shear resistance along diagonal tension crack

The first step in the development of the proposed closed-form shear resistance model is to derive the mean shear stress that can be resisted along the diagonal tension crack (τ_R) by aggregate interlock (τ_{ci}) and stirrups (τ_s). These stresses are derived using the MCFT which allows to determine the shear resistance for each of the failure modes described previously. The resistance to crack sliding is equal to the shear at the load step where the aggregate interlock at the crack (τ_{ci}) is equal to the maximum aggregate interlock ($\tau_{ci,max}$). The resistance to crushing in the compression fields is equal to the shear at the load step where the stress in the compression field (σ_2) corresponds to the maximum compression stress ($\sigma_{2,max}$).

The resistance for each of these failure modes has been determined using the MCFT for different combinations of parameters (Table 1). Although the concrete cylinder compressive strengths are assumed to vary between $f_{cm} = 40$ N/mm^2 and $f_{cm} = 100$ N/mm^2, the intermediate strengths of $f_{cm} = 60$ and $f_{cm} = 80$ N/mm^2 are also considered. This is because when using the MCFT, d_{max}, which is the maximum aggregate size, is linearly reduced from its actual value at $f_{cm} = 60$ N/mm^2 to zero at $f_{cm} = 80$ N/mm^2. This reduction takes into account that for higher strength concrete the cracks run through the aggregates due to the strong paste, resulting in a lower contribution of aggregate interlock.

Fixed values have been used for a number of other parameters. In regions without flexural cracks, the longitudinal strains in the web (ε_x) will be slightly less than zero. Since the longitudinal strain will not vary much

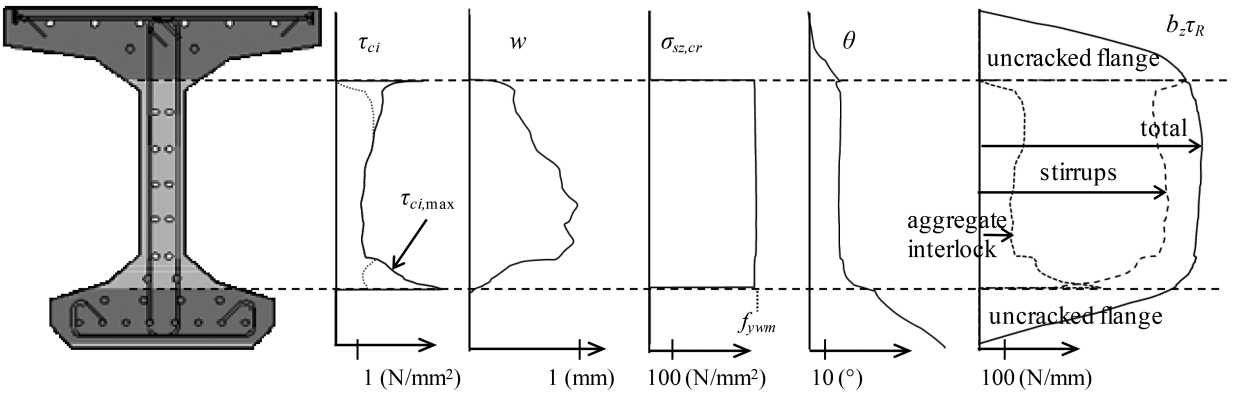

FIGURE 5 Contribution of shear transfer mechanism at failure of experiment HCP1TE[15]

f_{cm}	f_{ywm}	ρ_w	ε_x	d_{max}	s_θ
N/mm²	N/mm²	%	mm/m	mm	mm
40, 60,80, 100	250, 600	0.10, 0.25, 0.50, 0.75, 1.00	0	31.5	300

TABLE 1 Considered parameters for proposed model

over the region without flexural cracks, the shear resistance will also be approximately constant and the moment will have no significant influence on the location of failure. For simplicity, zero longitudinal strain will be assumed to derive the shear resistance for the regions without flexural cracks. Moreover, a diagonal cracking spacing s_θ of 300 mm is considered as a conservative assumption for elements that contain both transverse and longitudinal reinforcement. A fixed value for d_{max} of 31.5 mm was used, since this was used as standard in bridges in the Dutch Highway network that were designed before the 1974 design code[16] came into effect. In the Section 5, the effect of the presence of smaller maximum aggregate sizes on the accuracy of predictions will be investigated to clarify whether the proposed model can also be applied for beams with a smaller maximum aggregate size. Considering the number of parameters of Table 1, the resistances were determined for 40 combinations of parameters per failure mode.

The shear resistance is equal to the highest resistance of both failure modes. This can be explained considering a membrane element where the crack is just beginning to slip ($\tau_{ci} = \tau_{ci,max}$). When the shear strain increase further at the next load steps, two opposite phenomena occur: (i) by the decreasing angle of the cracks, a higher number of stirrups will be activated, increasing the shear that can be transferred by the stirrups, while (ii) the crack width will increase, reducing the shear that can be transferred by aggregate interlock. If the shear transfer by aggregate interlock decreases faster than the shear transfer by the stirrups increases, then crack sliding will be governing. If the contribution of the stirrups increases faster than the aggregate interlock decreases, then ultimately crushing in the compression field will be governing ($\sigma_2 = \sigma_{2,max}$).

Figure 6 shows τ_R that was found from the MCFT calculations for $f_{cm} = 60$ N/mm² and $f_{cm} = 80$ N/mm² and for different values of ψ which is defined as $\rho_w f_{ywm}/f_{cm}$. The resistance associated with crack sliding is plotted with black circles and the resistance associated with crushing in the compression field is plotted with gray diamonds. The shear resistance is equal to the highest resistance of both failure modes. For $f_{cm} = 60$ N/mm² crack sliding is found to be the highest and thus governing failure mode for zero longitudinal strain, independently of ψ (this is also the case for $f_{cm} = 40$ N/mm²). For $f_{cm} = 80$ N/mm² it is also possible that crushing in the compression field becomes the governing failure mode for the condition of zero longitudinal strain (this is also the case for $f_{cm} = 100$ N/mm²). This is due to the phenomenon that for $f_{cm} \geq 80$ N/mm² the maximum aggregate interlocking decreases as the cracks run through the aggregates and thus the resistance to crack sliding decreases. As a result, crushing the concrete turns out to be the highest and thus governing failure mode for these higher strengths of concrete for higher values of ψ.

The intent of the proposed model is to be able to determine approximately the same resistance as that found with a full MCFT analysis, but in a much simpler way. Therefore, the resistance found using the MCFT at zero longitudinal strain has been approximated with closed-form equations. This prevents the need for extensive MCFT analyses for each considered cross section of each bridge assessed. The shear resistance at zero longitudinal strain along the diagonal tension crack (τ'_R) consists

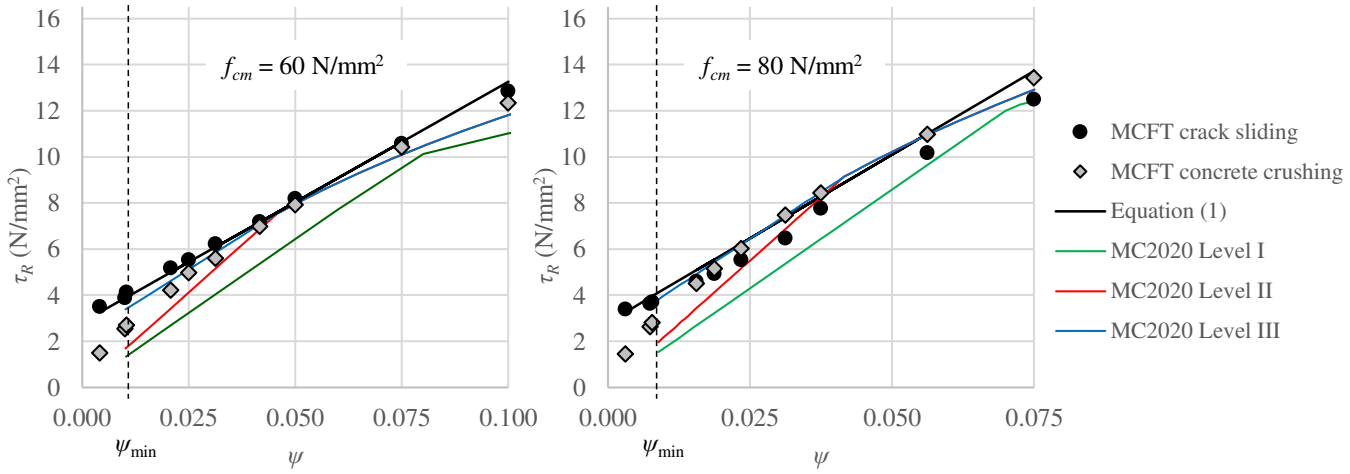

FIGURE 6 Shear resistance at $\varepsilon_x = 0$ versus ψ for $f_{cm} = 60$ N/mm^2 and $f_{cm} = 80$ N/mm^2

of a contribution of aggregate interlock (τ'_{ci}, which corresponds to $\beta\sqrt{f_{cm}}$) and the contribution of the stirrups (τ'_s, which corresponds to $\rho_z f_{ywm} \cot\theta$), as shown by Equation (1). The apostrophe is introduced for parameters that are related to the region without flexural cracks.

$$\tau'_R = \tau'_s + \tau'_{ci} = \rho_w f_{yw} \cot\theta + \beta\sqrt{f_{cm}} \quad (1)$$

To derive an equation for the contribution of aggregate interlock, a linear equation $\beta = ea + b\psi$ was assumed. The parameters a and b define a linear relation for β, for $f_{cm} \leq 60$ N/mm^2. The parameter e takes into account the decrease in aggregate interlock contribution for $f_{cm} \geq 80$ N/mm^2. To derive an equation for the contribution of stirrups, a linear equation $\theta = c + d\psi$ was assumed. The parameters c and d define a linear relation for θ. Initial values for a, b, c, d, and e were selected and the resistance according to the approximation equations was determined, which was then compared with the resistance according to the MCFT. Subsequently, the mean values of the ratio of both resistances and the associated coefficient of variation were determined for the 40 membranes. The values of a, b, c, d, and e were then adjusted until the mean value of the ratio of the resistances equals unity and a minimum coefficient of variation was found (which was ultimately 4%). This resulted in values for a, b, c, d, and e of 0.38, −2.5, 26, 0.0, and 0.8, respectively. In this way, the equations $\beta = 0.38–2.5\psi$ and $\beta = 0.30–2.5\psi$ are found for, respectively, $f_{cm} \leq 60$ N/mm^2 and $f_{cm} \geq 80$ N/mm^2. Moreover, a fixed crack angle θ is found of 26°. The resistances resulting from these equations are also shown in Figure 6 as a solid black line. This figure shows that the resistance predicted with the approximation equations agrees well with the shear resistance found with the MCFT, which is the maximum of the resistances to crack sliding (black circles) and concrete crushing (gray diamonds). The approximation equations for τ'_R will be used in the proposed model.

4.2 | Effective shear depth

The second step in the development of the proposed closed-form shear resistance model is to relate τ'_R to the shear force that can be resisted (V'_R). The way in which τ_{ci}, τ_s, and τ_{uncr} can be related to the shear forces is described in Section 2. In the proposed model, the shear resistance is simply determined by multiplying τ'_R by the web width (b_w) and a parameter defined as the effective shear depth z' (Figure 7). The effective shear depth which is used in the proposed model is derived based on the following assumptions:

- Failure occurs in the web. It is noted that while failure occurs in the web, the flanges may contribute significantly to the shear resistance V'_R (Figures 2 and 5).
- In regions without flexural cracks, the shear resistance of the web ($V'_{R,w}$) is equal to the maximum shear stress at zero longitudinal strain (τ'_R), multiplied by web height (h_w) and width of the web (b_w). This assumption is supported by Figures 2 and 5 which show that, at failure, the shear stress is evenly distributed over the height of the web and is approximately the same for the uncracked parts of the web as for the uncracked part of the web.
- The linear elastic stress distribution is representative for the distribution of the shear force at failure between the web and the flanges.

The effect of these assumptions will be examined at the end of this section by comparing the shear resistance

according to *Response* and the proposed model for various cross-sections.

Based on the above assumptions, the total shear resistance for a beam in the regions without flexural cracks (V'_R) can be found by increasing the resistance of the web ($V'_{R,w} = \tau'_R\, h_w\, b_w$) by the shear forces transmitted by the uncracked flanges. The proposed model accounts for this increase by replacing the web height (h_w) with the effective shear depth (z') as shown in Figure 7.

Given the assumption of linear elasticity, the distribution of shear stresses depends only on the geometric properties of the cross-section. Based on this assumption the ratio of the total shear force (V'_R) and the shear force transferred by the web ($V'_{R,w}$) can be determined analytically. The effective shear depth z' can then be found by dividing V'_R by $V'_{R,w}$ and multiplying this ratio by the height of the web h_w (in formula form: $z' = h_w\, V'_R/V'_{R,w}$). In this way, the effective shear depth z' was determined as ratio of h for different relative combinations of the geometric properties (Table 2).

For all investigated combinations, heights of the straight top flange ($h_{tf,str}$) are taken between 0.05 and 0.30 times the beam height (h) in steps of 0.05 h. For the web width (b_w), widths between 0.1 and 0.3 times the width of the top flange (b_{tf}) have been used (using 0.2 as a base value). In principle, the same width of the top flange and bottom flange (b_{bf}) is assumed, but as a variant, the width of the bottom flange is taken to be equal to 0.30 times the width of the top flange. This variant has been combined once, assuming equal heights of the top flange and bottom flanges ($h_{bf,str}$), which is typically for an edge girder of a box-girder bridge, and once with a height of the bottom flange that is three times as high as the height of the top flange, which is typically for a bulb T-girder. The presence of skew flanges was also investigated, for a height of the skew flanges ($h_{tf,skw}$) equal to the height of the top flange and a width equal to the flange width.

The results of the parameter study are shown in Figure 8. On the vertical axis, the calculated effective shear depth is shown as ratio of the height of the girder. The half of the summed height of the straight flanges is shown on the horizontal axis, to which a quarter of the summed height of the skew flanges has been added (if present). All considered combinations of geometric parameters show a comparable trend. The effective shear depth was found to depend mainly on the relative height of the straight and skew flanges. The relative width of the flanges did not significantly affect the effective shear depth. The mean of the lines found can be approximated by using an effective shear depth z' as defined in Equation (2), below. For a symmetrical I-beam with straight flanges, z' is simply the beam height minus the flange height. The ratio of z' and h found with this equation is also shown in Figure 8 (black solid line). Although the line for z'/h found with Equation (2) differs slightly from the other lines, the way of formulating is attractive because of its simplicity.

$$z' = h - (h_{tf,str} + h_{bf,str})/2 - (h_{tf,skw} - h_{bf,skw})/4 \quad (2)$$

The proposed equation for the effective shear depth is evaluated by comparing the resistance according to *Response* (which integrates the shear stresses over z and b_z) and the proposed model using Equation (2). Since it is not the intention to evaluate τ'_R, the resistance for the proposed model is determined based on the τ'_R at mid-depth as follows from the *Response* analyses. For this analyses, 26 cross-sections were used that correspond to beams from different series of experiments.[14,15,17,18] A mean ratio of the resistance according to *Response* and the proposed

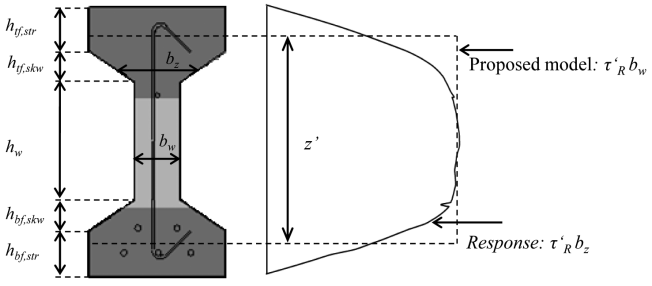

FIGURE 7 Distribution of shear stress times the cross-sectional or web width

TABLE 2 Considered geometric properties to determine the effective shear depth

	I-girder with small web	I-girder with wide web	Edge girder of box girder	Bulb T-girder	I-girder with skew flanges
$h_{tf,str}/h$	0.05–0.30	0.05–0.30	0.05–0.30	0.05–0.30	0.05–0.30
$h_{tf,str}/h_{bf,str}$	1	1	1	3	1
$h_{tf,skw}/h_{tf,str}$	0	0	0	0	1
b_w/b_{tf}	0.1	0.3	0.2	0.2	0.2
b_{bf}/b_{tf}	1	1	0.3	0.3	1

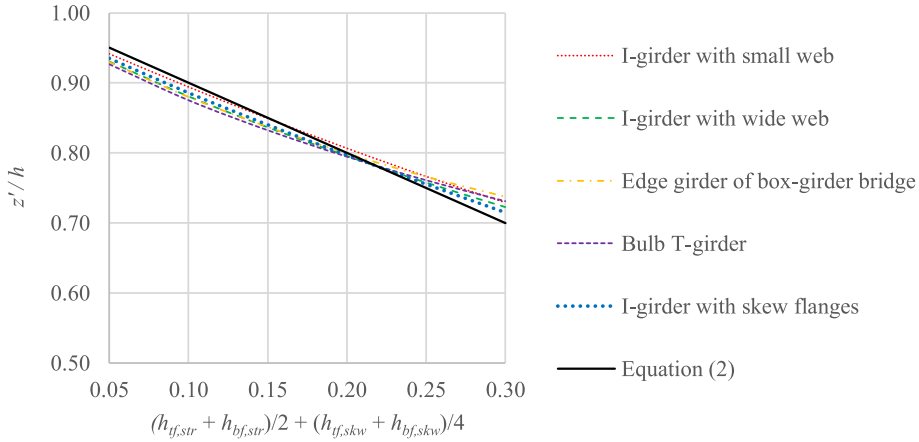

FIGURE 8 Ratio of the effective shear depth and beam height for different combinations of geometric properties

model using Equation (2) was found of 0.99 with an associated coefficient of variation of 2%. Apparently, the assumptions used to derive the equation for the effective shear depth, hardly affects the predicted resistance compared with the more advanced *Response* analysis.

4.3 | Proposed closed-form RBK-model

The proposed closed-form shear resistance model is referred to as RBK-model, after the guideline in which this model will be included (which is the "Richtlijnen Beoordeling Kunstwerken", abbreviated as RBK[2]). The RBK-model for the shear resistance in regions without flexural cracks corresponds to Equation (3). This equation is found by multiplying τ'_R, according to Equation (1), by b_w and z' according to Equation (2). The equation can be used for beams with a shear reinforcement ratio up to 1% (Table 1).

$$V'_{R,\mathrm{RBK}} = \beta \sqrt{f_{\mathrm{cm}}}\, b_w z' + A_{\mathrm{sw}}/s f_{\mathrm{ywm}}\, z' \cot\theta \qquad (3)$$

The shear resistance in regions without flexural cracks $V'_{R,\mathrm{RBK}}$ can be determined using $\theta = 26°$, $\beta = 0.38–2.5\psi$ for $f_{\mathrm{cm}} \leq 60$ N/mm^2, $\beta = 0.30–2.5\psi$ for $f_{\mathrm{cm}} \geq 80$ N/mm^2. In these equations, ψ equals $\rho_w f_{\mathrm{ywm}}/f_{\mathrm{cm}}$. The model is applicable if the tensile force in the most tensioned flange is lower than the resistance of the flange to cracking. Thus, the model is still applicable when shallow flexural cracks are present in the flange, but the flange is not yet completely cracked.

5 | VALIDATION OF THE PROPOSED RBK-MODEL

To validate the RBK-model, a database of experiments from the literature of prestressed beams with stirrups that failed in shear has been compiled.[9] Experiments from this database were considered suitable for the validation (i) if they failed in the regions without flexural cracks, (ii) if they could resist additional shear after diagonal tension cracking and (iii) if the shear span to depth ratio was larger than 2.5. Ultimately, 21 experiments were selected from five test series (Table 3), consisting of both simply and continuously supported beams, beams with posttensioned and pretensioned prestressing steel and beams with straight, draped and curved geometries of the prestressing steel. The shear reinforcement ratio ρ_w varied between 0.06% and 0.79%, the mean value of concrete cylinder compressive strength f_{cm} varied between 28 and 91 N/mm^2 and the mean yield strength of shear reinforment f_{ywm} varied between 298 and 585 N/mm^2. The accuracy of the RBK-model has been determined by dividing the experimentally found resistance ($V'_{R,\mathrm{exp}}$) and the predicted resistance ($V'_{R,\mathrm{model}}$ or $V'_{R,\mathrm{RBK}}$). For the 21 selected experiments, a mean value of the test-to-predicted shear resistance ratio was found of 1.33 with an associated coefficient of variation 15% (Table 3).

The assumption of a d_{max} of 31.5 mm leads to an overestimation of the predicted resistance because lower values of d_{max} were used for the experiments. On the other hand, when deriving the RBK-model a diagonal crack spacing s_θ of 300 mm has been conservatively assumed, which leads to an underestimation of the predicted resistance for the experiments. To investigate the effect of these both assumptions on the accuracy, the maximum shear stress that can be resisted was also determined by using the MCFT and explicitly taking into account d_{max} and s_θ. For this examination, s_x is equalized to the vertical distance between the bars in longitudinal direction at mid-depth and s_z is equalized to the center to center distance of the stirrups. Using this approach, the mean value of the test-to-predicted shear resistance ratio decreased from 1.33 to 1.23 and the corresponding coefficient of variation from 15% to 13% (Table 3). The effect of the overestimation of d_{max} was found to be more limited

TABLE 3 Accuracy of models for 21 experiments with $a/d > 2.5$

Research	Experiment	$V_{R,exp}$		$V_{R,exp}/V_{R,model}$		
–	–	kN		–		
				Closed-form RBK-model		
			d_{max} mm	Assuming $s_0 = 300$ mm and $d_{max} = 31.5$ mm	Taking into account s_0 and d_{max}	MC2010 Level III
Elzanaty et al.[17]	cw10	175	12.7	1.38	1.28	1.27
	cw11	158	12.7	1.26	1.26	1.21
	cw12	142	12.7	1.23	1.19	1.18
	cw13	184	12.7	1.45	1.31	1.33
	cw14	189	12.7	1.19	1.07	1.13
	cw15	152	12.7	1.19	1.14	1.09
	cw16	188	12.7	1.48	1.33	1.29
Choulli[15]	HCP1TE	796	12.0	1.65	1.45	1.52
	HCP1TW	746	12.0	1.55	1.36	1.42
	HAP1TE	648	12.0	1.31	1.15	1.21
	HAP1TW	749	12.0	1.51	1.32	1.40
Hanson[14]	FX1A	168	19.1	1.56	1.43	1.56
	FX1B	144	19.1	1.33	1.22	1.34
	F4B	171	19.1	1.64	1.50	1.65
	F5B	145	19.1	1.48	1.34	1.52
Rupf et al.[10]	SR23	275	16.0	1.02	0.89	1.08
	SR25	324	16.0	1.14	1.05	1.22
	SR26	293	16.0	1.07	0.97	1.17
	SR27	441	16.0	1.25	1.17	1.21
Xie[19]	lb2	172	10.0	1.21	1.26	1.17
	lb10	215	10.0	1.04	1.09	1.01
Mean				1.33	1.23	1.29
CoV (%)				15	13	13

than the effect of the conservatively assumed diagonal crack spacing. Therefore, the proposed model can also be applied for beams with smaller values of d_{max}.

The conservatively assumed diagonal crack spacing can be regarded, to some extent, as an explanation for the conservativeness of the predicted resistance. However, the main explanation for the conservative predictions seems to lie in the disregard of direct load transfer. This can be seen in Figure 9, which shows the ratio of $V_{R,exp}$ and $V_{R,model}$ as a function of the shear span to effective depth ratio (a/d). In this figure, five experiments with an a/d <2.5 were added to the 21 selected experiments to get a more complete picture of the trend. This figure shows that the predictions become less conservative for lower values of a/d. It is plausible that for these lower values of a/d, more load will be transferred directly to the support.

Finally, with regard to validation, it should be noted that with empirical models, which are still often used in practice, there is a risk that new experimental research will yield insights that make it necessary to adapt the model. This risk does not exist with the RBK-model because it is based entirely on the MCFT without calibrating the model with experimental data.

6 | COMPARISON OF THE RBK-MODEL WITH THE MODEL CODE 2010 MODELS

Figure 6 shows not only the shear resistance τ_R according to the RBK-model, but also the shear resistance according to three approaches of the MC2010. The mean resistance according to the MC2010 models are determined by using

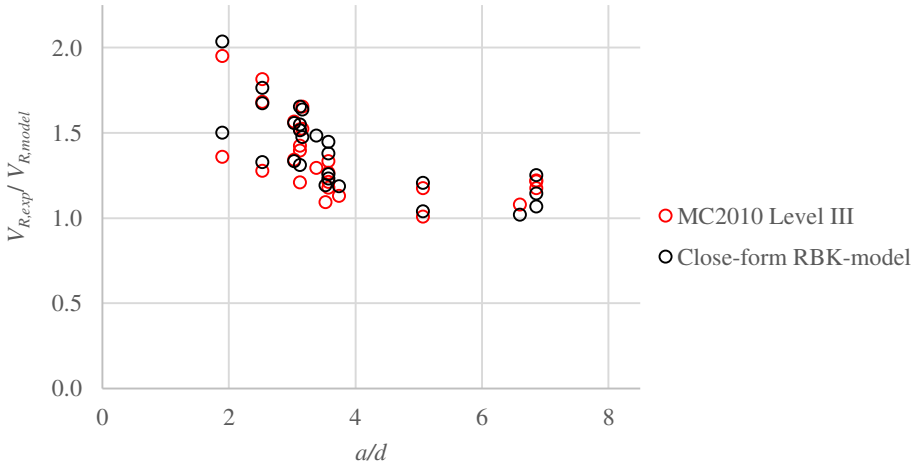

FIGURE 9 $V_{R,\exp}/V_{R,\text{model}}$ as a function of a/d

the equations according to the MC2010 with partial factors for concrete (γ_c) and steel (γ_s) of unity and by replacing the characteristic material properties by the mean material properties. For the comparison of the models, the ψ (in contrast to the graph 7.3-11 in the MC 2020, a factor is used without the brittleness factor η_{fc}) is limited to parameters considered to derive the proposed RBK-model (Table 1). The figure shows that the level I approach (presenting the variable angle truss model) and the level II approach (based on the generalized stress field approach) result in a lower resistance than that found with the MCFT. However, for the level III approach (based on the Simplified Modified Compression Field Theory), the predicted resistance agrees well with the resistance found according to the MCFT. The agreement is similar to that found with the RBK-model. This is not surprising as both the RBK and Level III models are based on the MCFT.

The first considered value for ψ in the graphs for the MC2010 models is $\psi_{\min}$. This concerns the value of ψ where the shear reinforcement ratio ρ is equal to its minimum $\rho_{\min}$. This $\rho_{\min}$ is required "to ensure that failure does not occur immediately upon shear cracking and truss action can develop" (art 7.13.5-2 of the MC2010). The amount of shear reinforcement when using $\rho_{\min}$ must therefore ensure that the resistance of an element with shear reinforcement is higher than the element without shear reinforcement. According to the MC2010, $\rho_{\min}$ is equated to $0.08\sqrt{f_{ck}}/f_{yk}$. However, in regions without flexural cracks of elements without shear reinforcement, the shear resistance is equal to the resistance to shear tension failure. This resistance is largely determined by the compressive stresses due to prestressing, especially when these are significant.[4,5,9] Since this parameter is missing in the given equation for $\rho_{\min}$, this equation it is not suitable for areas without flexural cracks. For assessing existing structures, the shear resistance can also simply be determined from the maximum of the resistance of the element with and without shear reinforcement, without considering $\rho_{\min}$. The graph in Figure 6 for the RBK-model is not limited to $\rho_{\min}$, so that this comparison is also possible for lower values of ρ.

Although the graphs (Figure 6) show that the predicted failure mode according to the MC2010 (crack sliding up to the kink in the graph and concrete crushing from the kink in the graph) does not always correspond to the prediction according to the MCFT (the highest resistance of both failure modes), the trend in failure modes is well described by the MC2010. The RBK-model, on the other hand, describes both failure modes with only one equation which simplifies the application of the RBK-model in practice.

The accuracy of the proposed RBK-model has been compared with the MC2010 Level III approach. Of the three possible levels of approximation, level III is chosen as the reference for the MC2010, despite requiring the use of many equations and iteration steps. This choice was made because this approximation will result in the least conservative predicted shear resistance (Figure 6). For the 21 experiments, a mean value of the test-to-predicted shear resistance ratio was found of 1.29 with an associated coefficient of variation 13% (Table 3).

When comparing the determination of the shear resistance for both models, the following observations can be made:

- Using the many equations and iteration steps associated with the level III approach, does not lead to a significant increase in accuracy compared with the proposed closed-form RBK-model.
- The shear resistance according to the MC2010 model turned out to be slightly less conservative than found with the RBK-model. This is because the effective shear depth based on the effective depth of the prestressing and reinforcing steel is on average higher than based on the concrete properties. Since the steel

is in the uncracked flanges, the location does not determine the height of the crack over which aggregate interlock occurs and the stirrups are activated. The observation that the shear resistance is predicted less conservatively using the MC2010 is therefore not based on a physical explanation but can be regarded as a coincidence.

- Figure 9 shows that the predictions according to both models become less conservative with higher values of the ratio between shear stress and effective depth. This is not surprising because both models are based on the MCFT and do not consider direct load transfer.
- The proposed RBK-model is derived for shear reinforcement ratios up to 1%. The MC2010 Level III approach can on the other hand also be used for higher shear reinforcement ratios.
- Both the RBK-model and the MC2010 level III approach do not relate the shear resistance to d_{max} or the diagonal crack spacing. Although this simplification will affect the accuracy of the predicted shear resistance to some extent, it is attractive because it simplifies the application of the models.

7 | CONCLUSIONS

This article proposes a closed-form model, referred to as the RBK-model, that can be used to determine the shear resistance in regions without flexural cracks. The RBK-model is easy-to-use in engineering practice as no iterations are necessary. The use of the RBK-model is simplified even further because two possible shear failure modes have been described with only one equation. The shear resistance can be determined with the RBK-model as accurately as with the most comprehensive level III approach of the MC2010.

A simple equation for effective shear depth is included in the RBK-model, which is suitable for regions without flexural cracks. Unlike the MC2010, the effective shear depth is not based on the location of the reinforcing and prestressing steel because these have no influence on the shear resistance in the regions without flexural cracks. The effective shear depth is instead based on the cross-sectional properties of concrete. In this way, the transfer of the shear force through the uncracked flanges is taken into account in a physically logical way.

DATA AVAILABILITY STATEMENT

The data that support the findings of this study are openly available in the repository of the Delft University of Technology at https://doi.org/10.4233/uuid:e3615629-cfe2-4fc7-920d-5bc2e776e7c5.

ORCID

Marco A. Roosen https://orcid.org/0000-0002-7466-6900

REFERENCES

1. European Committee for Standardisation (CEN). NEN-EN 1992-1-1 Eurocode 2: Design of concrete structures—Part 1-1: General rules and rules for buildings. CEB, EN 1992-1-1, Brussels, 2005
2. Rijkswaterstaat (RWS). Richtlijnen beoordelen kunstwerken (RBK), RTD1006, RBK1.1. 2013
3. Walraven J.C. Background document for prENV 1992-1-1: 2002, Report, Delft University of Technology. 2002
4. MacGregor JC, Sozen MA, Siess CP. Strength and behavior of prestressed concrete beams with web reinforcement. Urbana, Illinois: University of Illinois; 1960.
5. American Concrete Institute (ACI). ACI Committee 318: building code requirements for structural concrete (ACI 318-08) and commentary. USA: Farmington Hills, MI; 2008.
6. Fédération Internationale du Béton (fib). Model Code 1990, fib Model Code for Concrete Structures 1990, Thomas Telford, 1993
7. Fédération Internationale du Béton (fib). Model Code 2010—final draft, vol.1, Bulletin 65, and vol. 2, Bulletin 66, Lausanne, Switzerland. 2013.
8. CSA: Canadian Highway Bridge Design Code CAN/CSA-S6-06 and commentary, Canadian Standard Association, 2006
9. Roosen MA. Shear resistance of prestressed girders in regions without flexural cracks. Delft: Delft University of Technology; 2021. https://doi.org/10.4233/uuid:e3615629-cfe2-4fc7-920d-5bc2e776e7c5
10. Rupf M, Ruiz MF, Muttoni A. Post-tensioned girders with low amounts of shear reinforcement: shear strength and influence of flanges. Eng Struct. 2013;56:357–71. https://doi.org/10.1016/j.engstruct.2013.05.024
11. Sigrist V Assessment of Structural Concrete Members using the fib ModelCode 2010 Shear Provisions. Proceedings of the IABSE Spring Conference 2013;534–5. https://doi.org/10.2749/222137813806521379
12. Bentz E.C. Sectional analyses of reinforced concrete members. University of Toronto 2000
13. Vecchio FJ, Collins MP. The modified compression-field theory for reinforced concrete elements subjected to shear. ACI J. 1986;83:219–31.
14. Hanson JM. Ultimate shear strength of prestressed concrete beams with web reinforcement. Bethlehem: Lehigh University; 1964.
15. Choulli Y, Mari AR, Cladera A. Shear behaviour of full-scale prestressed I-beams made with self-compacting concrete. Mater Struct. 2008;41:131–41. https://doi.org/10.1617/s11527-007-9225-1
16. Nederlands Normalisatie Instituut (NEN). Voorschriften Beton 1974. NEN3861. 1974.
17. Elzanaty AH, Nilson AH, Slate FO. Shear capacity of prestressed concrete beams using high-strength concrete. J Am Concr Inst. 1986;83:359–68.
18. Leonhardt F, Koch R, Rostásy S. Schubversuche an Spannbetonträgern. Deutscher Ausschuss für Stahlbeton. 1973;227:1–179.
19. Xie L. The influence of axial load and prestress on the shear strength of web-critical reinforced concrete elements. Toronto: University of Toronto; 2009.

AUTHOR BIOGRAPHIES

Marco A. Roosen, Dutch Ministry of Infrastructure and Water Management, Rijkswaterstaat, Utrecht, The Netherlands.

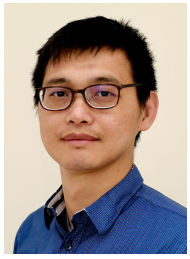

Yuguang Yang, Delft University of Technology (TU Delft), Delft, The Netherlands.

Cor van der Veen, Delft University of Technology (TU Delft), Delft, The Netherlands.

Dick G. Schaafsma, Dutch Ministry of Infrastructure and Water Management, Rijkswaterstaat, Utrecht, The Netherlands.

Max A. N. Hendriks, Norwegian University of Science and Technology (NTNU), Trondheim, Norway.

How to cite this article: Roosen MA, Yang Y, van der Veen C, Schaafsma DG, Hendriks MAN. A closed-form shear resistance model for regions of prestressed beams without flexural cracks. Structural Concrete. 2022;23:1304–15. https://doi.org/10.1002/suco.202100695